

# Irreversibility, Mechanical Entanglement and Thermal Melting in Superconducting Vortex Crystals with Point Impurities

Deniz Ertas and David R. Nelson

Department of Physics, Harvard University, Cambridge, Massachusetts 02138

(April 18, 2018)

We discuss the onset of irreversibility and entanglement of vortex lines in high  $T_c$  superconductors due to point disorder and thermal fluctuations using a simplified cage model. A combination of Flory arguments, known results from directed polymers in random media, and a Lindemann criterion are used to estimate the field and temperature dependence of irreversibility, mechanical entanglement and thermal melting. The qualitative features of this dependence, including its nonmonotonicity when disorder is sufficiently strong, are in good agreement with recent experiments.

## Introduction

The physics of vortex matter in high temperature superconductors (HTSC) has generated considerable interest since these materials were discovered about a decade ago [1]. The magnetic flux lines in a clean material prefer to sit on the sites of a triangular lattice forming an Abrikosov solid below the superconducting transition temperature  $T_c$ . However, the combined effects of thermal fluctuations and various types of disorder, such as oxygen vacancies, columnar pins or twin boundaries, significantly alters the phase diagram, which is further complicated by typically large crystallographic anisotropies [2]. In fact, pinning of flux lines by disorder is important technologically, since the flux lines must be immobilized in order to eliminate dissipative losses associated with flux line motion. In this paper, we will focus on pinning by pointlike defects, such as oxygen vacancies. There are many recent studies in the literature that have considered other types of disorder [3,4].

It is well known that even an arbitrarily small amount of point disorder is sufficient to disrupt the delicate long range translational order of the Abrikosov crystal [5]. However, the existence of a distinct “vortex glass” phase [6,7] at low temperatures (one which presumably contains dislocations and/or disclination defects) is still controversial. Indeed, experiments in which electron irradiation injects point disorder in twin-free  $\text{YBa}_2\text{Cu}_3\text{O}_{7-\delta}$  (YBCO) samples in amounts large enough to destroy the first order melting transition have failed to find a sharp vortex glass transition with universal exponents [8]. On the other hand, the presence of a stable, topologically ordered, i.e., dislocation-free, “Bragg glass” phase was recently suggested by various authors [9] at low magnetic fields [10] and temperatures in the presence of weak point disorder. We will loosely refer to such a configuration as the “ordered phase”. When dislocations are absent, the interaction of a flux line (FL) with its neighbors can be approximated by an effective confinement potential that keeps the FL from wandering away, similar to the Einstein model of phonons in conventional crystals. We ap-

ply the Lindemann criterion to this “cage model” (where the confinement potential is approximated by a simple harmonic well) in order to investigate the combined effect of thermal fluctuations and point disorder. A similar model was used previously to investigate the effects of correlated disorder due to columnar pins in Ref. [3]. The discussion will focus primarily on  $\text{Bi}_2\text{Sr}_2\text{CaCu}_2\text{O}_{8+\delta}$  (BSCCO) crystals, where the large anisotropy confines transitions out of the hypothetical Bragg glass to easily accessible fields and temperatures. We seek to understand the following three phenomena observed by experiments (See Fig. 1):

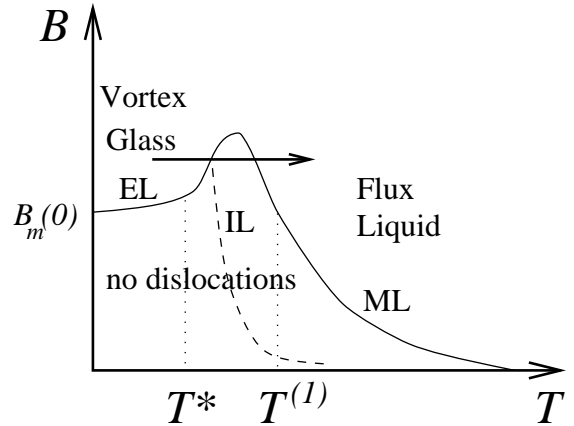


FIG. 1. Schematic phase diagram indicating the approximate location and shape of the irreversibility line (dashed) and the combined melting-entanglement line (solid). The arrow indicates the path taken for the situation depicted in Fig. 5.

(i) *The melting line (ML)* marks the loss of order in the FL system, and is widely believed to be a first-order thermodynamic phase transition, most notably marked by a finite jump in the magnetization as a function of both temperature and applied field [11].

(ii) *The irreversibility line (IL)* marks the cross-over when a sample falls out of equilibrium on laboratory time scales. It is typically determined by the onset of hystere-

sis in the magnetization curve, and is recently demonstrated to be separate from the melting line, provided that one excludes effects due to surface barriers [12].

(iii) *The entanglement line (EL)* has only been studied more recently and can be defined experimentally by a sudden increase in the critical current when the field is increased at low temperature [13]. Fairly independent of temperature, its driving mechanism may be the gradual proliferation of large dislocation loops favored by point disorder [9,14]. The onset of the large critical currents at low temperatures with increasing field coincides approximately with the field above which the intensity of Bragg peaks in neutron diffraction experiments suddenly decrease [15]. Unlike first order melting, these phenomena are not accompanied by a magnetization jump, suggesting a continuous phase transition or a crossover [13]. The proliferation of large scale dislocation loops would generate entanglement via their screw dislocation components (see Fig. 2), as suggested years ago by Wördenweber and Kes [16] and by Brandt [17] in the context of dimensional crossover. Provided line crossing barriers are large, such long wavelength entanglements would increase the effectiveness of pinning, similar to ideas about enhanced pinning in arrays of splayed columnar defects [18]. As the dislocations become denser with further increases in the field, vortex crossing angles will become large, flux cutting easier and critical currents should drop. The critical current in experiments does in fact gradually decrease with further increases in magnetic field [13], indicative of a gradual evolution to a decoupled regime of “superentangled” pancake vortices.

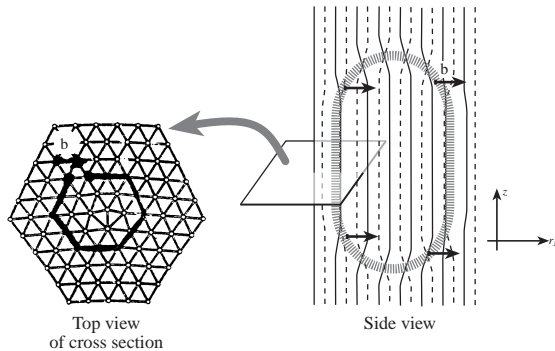


FIG. 2. Dislocation loop in a topologically ordered vortex crystal. Nucleation of dislocation pairs in a constant  $z$  cross-section (corresponding to the bottom of the loop) becomes more likely when the Lindemann criterion is reached. Dashed lines represent flux lines just behind the plane of the figure. Top view shows the Burgers' construction applied to a cross-section through the loop. dimensions.

Numerical evidence for this mechanical entanglement scenario has been provided by simulations of Gingras and Huse of a disordered XY model [14], where vortex rings play the role of dislocation loops in an Abrikosov lattice. These authors find evidence for a continuous phase transition to a defect free phase at low temperatures below

a finite disorder strength in three dimensions. In  $d = 2$ , the transition occurs only at vanishing disorder strength. To make connections with real vortex arrays, effects of disorder in a given sample are assumed to increase with increasing magnetic fields. Direct simulations of vortex arrays with point disorder in three dimensions by Ryu *et al.* [19] also support this picture, finding evidence for a proliferation of lines of disclination pairs (i. e., dislocations) above a critical field threshold [20].

Our model suggests a relatively simple scenario in which the melting, irreversibility and entanglement lines can be understood and connected in a way consistent with experimental observations. In this scenario, a sudden increase in intravalley energy barriers is responsible for the portion of the IL that lies within the ordered phase. The lines ML and EL in Fig. 1 are connected, and both signal the proliferation of dislocations. However, the primary mechanisms are different. The ML occurs at temperatures above the IL where point disorder is ineffective at pinning FLs. Melting is thus a competition between thermal fluctuations and interaction effects. The thermal melting line is only slightly perturbed from its position in the absence of disorder. However, at temperatures below the IL, disorder-induced wandering of the FL beyond the Lindemann criterion possibly causes the proliferation of *frozen-in* dislocations that give rise to a mechanically entangled configuration with a substantially increased critical current. This phenomenon, whether a crossover or a sharp continuous phase transition, results from a competition between interactions and the effects of point disorder.

For simplicity, let us assume that the average magnetic field  $B$  is along the  $c$ -axis of the sample. The Hamiltonian of a single FL whose configuration  $\mathbf{r}(z)$  fluctuates about the line  $\mathbf{r}(z) = \mathbf{r}_0$  can be written approximately as

$$\mathcal{H}[\mathbf{r}(z)] = \int_0^L dz \left\{ \frac{\tilde{\epsilon}}{2} \left( \frac{d\mathbf{r}}{dz} \right)^2 + V(\mathbf{r}(z), z) + \frac{k}{2} |\mathbf{r} - \mathbf{r}_0|^2 \right\}, \quad (1)$$

where  $\tilde{\epsilon} = \epsilon_0/\gamma^2$  is the line tension of the FL,  $\gamma^2 = m_z/m_\perp \gg 1$  is the mass anisotropy,  $\epsilon_0 = (\Phi_0/4\pi\lambda)^2$ , and  $k \approx \epsilon_0/a_0^2$  is the effective spring constant due to interactions with neighboring FLs, which are typically at a distance  $a_0 = \sqrt{\Phi_0/B}$ . This approximation to  $k$  requires  $B > H_{c1}$ , so that the vortices interact with a logarithmic potential at the nearest neighbor spacing. The probability of a particular vortex trajectory is proportional to  $\exp\{-\mathcal{H}[\mathbf{r}(z)]/k_B T\}$ . (The Boltzmann constant  $k_B$  will be suppressed henceforth.) The disorder potential  $V$  is assumed to have zero mean and short-range correlations

$$\langle V(\mathbf{r}, z) V(\mathbf{r}', z') \rangle = \Delta \delta_\xi^{(2)}(\mathbf{r} - \mathbf{r}') \delta(z - z'), \quad (2)$$

where  $\delta_\xi(r)$  is a delta function smeared out to the vortex core diameter  $\xi$ . It will be useful to define a dimensionless disorder parameter given by

$$\tilde{\Delta} = \Delta/(\epsilon_0^2 \xi^3). \quad (3)$$

In the *absence* of the cage potential ( $k = 0$ ), the model reduces to a directed polymer in a 2+1 dimensional random medium, which has been studied extensively [21]. At low temperatures, the FL makes transverse excursions

$$u_0^2(\ell) \equiv \langle |\mathbf{r}(z) - \mathbf{r}(z + \ell)|^2 \rangle \approx \xi^2 (\ell/\ell_c)^{2\zeta}, \quad \ell > \ell_c, \quad (4)$$

and the energy barriers between low-energy configurations grow as [22]

$$\mathcal{U}_{p0}(\ell) \approx T^* (\ell/\ell_c)^{2\zeta-1}. \quad (5)$$

A Flory-type argument [23], combined with the known value of  $\zeta \approx 5/8$  [21] gives

$$\ell_c \approx (\xi/\gamma)(\tilde{\Delta}\gamma)^{-1/3}, \quad (6)$$

$$T^* \approx (\xi\epsilon_0/\gamma)(\tilde{\Delta}\gamma)^{1/3}. \quad (7)$$

At shorter length scales, where it is justified to expand the random potential in Eq.(1) about  $\mathbf{r} = \mathbf{r}_0$ ,

$$V(\mathbf{r}(z), z) \approx V(\mathbf{r}_0, z) + (\mathbf{r}(z) - \mathbf{r}_0) \cdot \nabla_{\mathbf{r}} V(\mathbf{r} = \mathbf{r}_0, z), \quad (8)$$

the fluctuations are given by the Larkin-Ovchinnikov formula

$$u_0^2(\ell) \approx \xi^2 (\ell/\ell_c)^3, \quad \ell < \ell_c. \quad (9)$$

However, this regime is not relevant to Lindemann discussions of entanglement provided that  $c_L a_0 > \xi$ , and will be ignored henceforth. ( $c_L$  is the Lindemann constant, see below.) Thermal noise is ineffective at depinning the FL from individual pinning centers as long as the magnitude of thermal fluctuations are smaller than quenched fluctuations at the crossover length scale, i.e. when  $u_{th}^2(\ell_c) = T\ell_c/\tilde{\epsilon} \ll \xi^2$ , or equivalently when  $T \ll T^*$ . At higher temperatures, the excursions of the FL at short distances are determined mainly by thermal noise. However, the scaling of transverse fluctuations is still determined by point disorder when  $\ell > \ell_c(T)$ , where the temperature dependent crossover length scale is [2]

$$\ell_c(T) = \begin{cases} \ell_c, & T \ll T^*, \\ \ell_c \frac{T^*}{T} e^{c(T/T^*)^3}, & T^* \ll T, \end{cases} \quad (10)$$

where  $c$  is a constant of order unity. The sharp exponential increase of  $\ell_c(T)$  as  $T$  exceeds  $T^*$  is caused by thermal smearing of the disorder potential at the marginal dimension  $d = 3$ . Transverse fluctuations of the FL are

$$u_0^2(\ell) \approx \begin{cases} \xi^2 (\ell/\ell_c)^{5/4}, & T < T^*, \ell > \ell_c, \\ \frac{T}{\tilde{\epsilon}} \ell, & T > T^*, \ell < \ell_c(T), \\ \frac{T}{\tilde{\epsilon}} \ell_c(T) \left[ \frac{\ell}{\ell_c(T)} \right]^{5/4}, & T > T^*, \ell > \ell_c(T), \end{cases} \quad (11)$$

and typical energy barriers are

$$\mathcal{U}_{p0}(\ell) \approx \begin{cases} T^* \left[ \frac{\ell}{\ell_c} \right]^{1/4}, & T < T^*, \ell > \ell_c, \\ T, & T > T^*, \ell < \ell_c(T), \\ T \left[ \frac{\ell}{\ell_c(T)} \right]^{1/4}, & T > T^*, \ell > \ell_c(T). \end{cases} \quad (12)$$

The main effect of the cage potential is to block transverse excursions of the FL beyond a confinement length  $\ell^* \approx \sqrt{\tilde{\epsilon}/k} = a_0/\gamma$ , which is obtained by balancing the tilting and confinement energies. Every time the vortex wanders a distance  $\ell^*$  along the  $z$ -axis, it is reflected back by the walls of the cage potential and must restart its thermal or disorder dominated random walk. Thus, the mean square displacement of the FL around its equilibrium position and the typical energy barriers are respectively given by

$$u^2(T) \approx u_0^2(\ell^*), \quad (13)$$

$$\mathcal{U}_p(T) \approx \mathcal{U}_{p0}(\ell^*). \quad (14)$$

The vortex line acts as if it were broken up into independent subsystems of length  $\ell^*$ . Similar arguments for the effect of interactions on point disorder and thermal fluctuations were given for flux *liquids* in Ref. [24].

### The Irreversibility Line

Using the results (10-14), let us investigate the phenomena described earlier in the context of this simple model. Naively, one would expect the IL to be associated with a sudden increase in energy barriers against the motion of individual FLs. When  $T \gg T^{(1)}$ , where  $T^{(1)}$  is defined by the condition

$$\ell_c(T^{(1)}) = \ell^*, \quad (15)$$

pinning centers do not offer a gain in the free energy of the FLs, and there are no barriers against FL motion. The slowest relaxation time of the FL in this regime is

$$\tau_0 \approx \frac{\eta}{k} = \frac{8\pi\lambda^2 a_0^2}{c^2 \xi^2 \rho_n}, \quad (16)$$

where  $\eta = \Phi_0 H_{c2}/(\rho_n c^2)$  [25] is the friction coefficient of the FL, and  $\rho_n$  is the resistivity of the normal electrons in vortex cores. When  $T$  drops into the range  $T^* < T < T^{(1)}$ , energy barriers grow rapidly and the relaxation time increases to

$$\tau(T) = \tau_0 e^{\mathcal{U}_p(T)/T} \quad (17)$$

$$\sim \tau_0 \exp \left\{ \left( \frac{\ell_c(T^{(1)})}{\ell_c(T)} \right)^{1/4} \right\}, \quad T^* < T < T^{(1)}. \quad (18)$$

Eventually, energy barriers saturate at  $T \approx T^*$ , resulting in

$$\tau(T) = \tau_0 \exp \left\{ \frac{T^*}{T} \left( \frac{\ell^*}{\ell_c} \right)^{1/4} \right\}, \quad T \ll T^*. \quad (19)$$

Thus, in a range of temperatures near  $T^*$ , the relaxation time increases rapidly to macroscopically long times. The irreversibility condition is satisfied when  $\log(\tau(T)/\tau_0)$  becomes fairly large. Upon further manipulation, this yields

$$B_{IL}(T) \approx \begin{cases} B_{IL}(T^*) \exp\{-2c(T/T^*)^3\}, & T > T^*, \\ B_{IL}(T^*)(T/T^*)^{-8}, & T < T^*. \end{cases} \quad (20)$$

### The Melting and Mechanical Entanglement Lines

In order to estimate where dislocations appear in the  $B - T$  phase diagram, we can employ a Lindemann criterion as follows:

$$u^2(T_m(B)) = c_L^2 a_0^2, \quad (21)$$

where  $c_L \approx 0.15 - 0.2$  is the phenomenological Lindemann constant [26]. Thus, for a given sample, the form of  $u^2(T)$  will determine the shape of the melting line. We next discuss various regimes in this function and the corresponding melting fields  $B_m(T)$ .

1.  $T \ll T^*$ : In this region, the Lindemann criterion (21) becomes

$$\xi^2(a_0 T^*/\gamma \xi^2 \tilde{c})^{5/4} = c_L^2 a_0^2. \quad (22)$$

Upon simple manipulation, this yields

$$B_m(0) \approx \frac{\Phi_0}{\xi^2} \left( \frac{\epsilon_0 \xi}{\gamma T^*} \right)^{10/3} c_L^{16/3}, \quad T \ll T^*. \quad (23)$$

Taking, as parameters for BSCCO,  $\xi = 20 \text{ \AA}$ ,  $\gamma = 100$ ,  $\epsilon_0 \xi = 1000 \text{ K}$ , and  $T^* = 10 \text{ K}$ ,  $c_L \approx 0.17$  leads to  $B_m(0) \approx 400 \text{ Gauss}$ , in reasonable agreement with experimental results [13]. Note that the results depend sensitively on the value of the roughness exponent  $\zeta \approx 5/8$  and the Lindemann constant  $c_L$ .

2.  $T^* < T < T^{(1)}$ : In this region, thermal fluctuations spread the vortex probability distribution and weaken the pinning effect of point disorder, but the relevant length scale at which the cage potential is seen is still determined by the anomalous wandering characteristics of point pinning. The result is

$$B_m(T) \approx B_m(0) \left( \frac{T^*}{T} \right)^{10/3} e^{\frac{2c}{3}(T/T^*)^3}, \quad T^* < T < T^{(1)}, \quad (24)$$

indicating an *increase* in the melting field with  $T$ .

3.  $T \gg T^{(1)}$ : In this region, the FL sees the cage potential before it has a chance to take advantage of point disorder, which is effectively smeared out and can be neglected as a first approximation. We then find the well-known portion of the melting line,

$$B_m(T) \approx \frac{\Phi_0 \epsilon_0^2 c_L^4}{\gamma^2 T^2}, \quad T^{(1)} \ll T. \quad (25)$$

Note that  $\epsilon_0$  has an implicit dependence on temperature, and the effective anisotropy parameter  $\gamma$  can depend on the amount of point disorder. The melting field is a decreasing function of temperature in this regime.

Combining these three regimes gives rise to a non-monotonic melting field  $B_m(T)$ , which is qualitatively depicted in Fig. 1. At the lower temperature side of this peak,  $B_m(T)$  lies below the irreversibility line, and configurations of the FL are effectively pinned by point disorder. Thus, it is more appropriate to regard the Lindemann criterion in this regime as a pointer to the onset of mechanical entanglement, rather than melting [27]. More sophisticated methods are needed to determine the nature (first or second order transition, or crossover) of this onset. The high temperature side of the curve corresponds to the more familiar and studied phenomenon of flux lattice melting, which was observed as a first-order thermodynamic phase transition. Finally, the nonmonotonic behavior disappears when the disorder is too weak, i.e. for  $T^* \lesssim c_L \xi \epsilon_0 / \gamma$ . The transition line observed recently by Khaykovich *et al.* [13] in highly anisotropic Bi-based HTSCs is in good qualitative agreement with our model.

### Numerical Results

In order to test the analytical results, we have numerically determined  $u^2(T)$  for various values of the magnetic field. The general procedure is outlined below, a more detailed discussion on Eqs. (26-28) can be found in Ref. [28].

The “weight” function for a FL starting from  $\mathbf{r}_i$  at  $z = 0$  and wandering across a sample of thickness  $\ell$  to position  $\mathbf{r}$  is given by

$$W(\mathbf{r}, \mathbf{r}_i; \ell) = \int_{\mathbf{r}'(0)=\mathbf{r}_i}^{\mathbf{r}'(\ell)=\mathbf{r}} \mathcal{D}\mathbf{r}'(z) \exp\{-\mathcal{H}[\mathbf{r}'(z)]/T\}, \quad (26)$$

which satisfies a Schrödinger-like equation with a time-dependent (“time  $\equiv z$ ”) potential,

$$\partial_z W(\mathbf{r}, \mathbf{r}_i; z) = \left[ \frac{T}{2\tilde{\epsilon}} \nabla_{\mathbf{r}}^2 - \frac{k}{2} |\mathbf{r} - \mathbf{r}_0|^2 - V(\mathbf{r}(z), z) \right] W(\mathbf{r}, \mathbf{r}_i; z). \quad (27)$$

For a given realization of point disorder, the weight function can thus be determined by discretizing and stepping this equation forward in the time-like parameter  $z$ . The probability distribution for the position of a FL at a height  $z$  which is far from the boundaries of a sample of thickness  $\ell$  is proportional to

$$P(\mathbf{r}; z) \propto \int d\mathbf{r}_i \int d\mathbf{r}_f W(\mathbf{r}_f, \mathbf{r}; \ell - z) W(\mathbf{r}, \mathbf{r}_i; z). \quad (28)$$

For a given realization of disorder, the weight function ratio  $W(\mathbf{r}, \mathbf{r}_i, z)/W(\mathbf{r}', \mathbf{r}_i; z)$  becomes independent of  $\mathbf{r}_i$  when  $z \gg \ell^*$  since the FL forgets its initial position after bouncing off of the confinement potential a few times. We have numerically confirmed that the starting position is indeed indistinguishable for  $z > 5\ell^*$ , in agreement with the argument above. Thus, the integral over initial and final positions in Eq. (28) can be eliminated by setting  $\mathbf{r}_i = \mathbf{r}_f = \mathbf{r}_0$ . (Alternatively, one could start from a uniform weight function.) Furthermore, the two weight functions that appear in Eq. (28) are statistically independent, since they traverse different portions of the sample. Taking advantage of these properties, we have determined  $P$  by multiplying two weight functions which were propagated through different samples by  $z = 5\ell^*$ . This probability distribution was used to determine the fluctuation amplitude, which was subsequently averaged over different realizations of disorder. Fig. 3 shows the results for the parameter values  $\tilde{\Delta} = \gamma = 1$ , for different values of the dimensionless field  $b \equiv B\xi^2/\Phi_0$ . In order to solve Eq. (27), each  $z$ -slice was discretized to a square lattice with lattice constant  $\xi$ , and consecutive  $z$ -slices were a distance  $\delta z = 0.05\xi/\gamma$  apart. The random potential  $V$  was determined independently at each site of the square lattice and had a correlation length of  $\xi/\gamma$  along the  $z$ -direction.

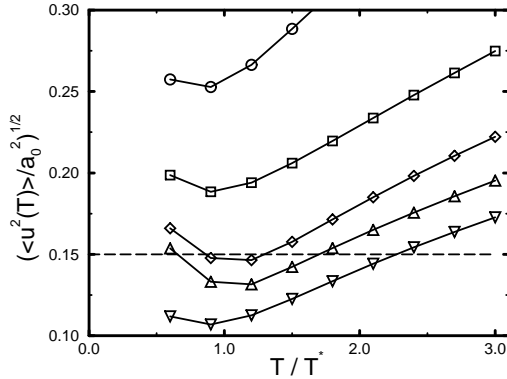


FIG. 3. Results of a transfer matrix computation of transverse fluctuations in the cage model. The curves represent temperature scans at  $b \equiv B\xi^2/\Phi_0 = 1/100$  (circles),  $1/400$  (squares),  $1/900$  (diamonds),  $1/1600$  (upwards triangles), and  $1/2500$  (downwards triangles). The parameters in this run were  $\tilde{\Delta} = \gamma = 1$ .  $c_L = 0.15$  is shown as a representative Lindemann constant.

While this method allows exact thermal averaging of fluctuations, obtaining the disorder average is much more difficult, as illustrated in Fig. 4. The spread of data points (each representing one realization of disorder) increases dramatically for  $T < T^*$ , when disorder becomes dominant. Ideally, disorder averaging should be done

over many more samples to achieve reliable results. Nevertheless, reentrant behavior can be deduced from the clear nonmonotonicity of the fluctuation amplitude as a function of temperature, as seen in Fig. 3. This feature can be understood qualitatively as follows (See Fig. 5): As the temperature is increased from  $T = 0$ , thermal fluctuations will initially act to blur the pinning centers, thus reducing their pinning strength and giving rise to a straighter FL with a smaller fluctuation amplitude. However, further increases in temperature eventually spread the FL, increasing the fluctuation amplitude.

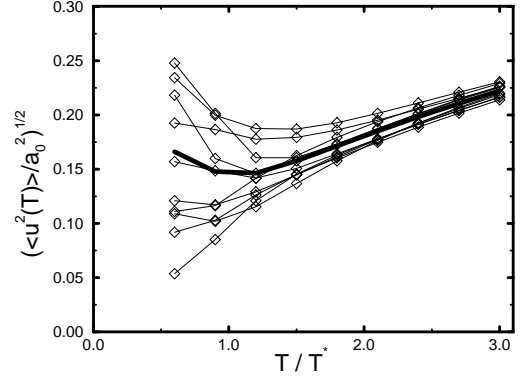


FIG. 4. Temperature scans of the 10 samples (thin lines) used to determine the disorder averaged fluctuation amplitude (thick line) for  $b = 1/900$ . The spread in data points increases significantly when  $T$  drops below  $T^*$ .

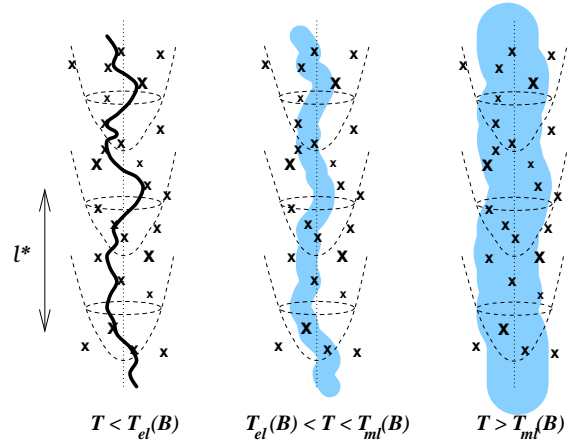


FIG. 5. Transverse fluctuations of a FL are minimized at an intermediate temperature (middle) due to the competition between point disorder and thermal noise. Reentrant behavior is possible if the Lindemann criterion is crossed during a temperature sweep (See Fig. 3).

## Discussion

In this paper, we have presented the results of a simple “cage model” for a FL embedded in a dislocation-

free vortex phase. The model describes the *relative* motion of a vortex with respect to the cage provided by its neighbors, and is thus insensitive to the long wavelength disorder fluctuations studied in Refs. [5–7,9]. An equivalent theory could presumably be constructed within the usual Debye phonon model by setting  $\langle |\mathbf{u}(\mathbf{r} + a_0 \mathbf{e}_1) - \mathbf{u}(\mathbf{r})|^2 \rangle = c_L^2 a_0^2$ , where  $\mathbf{e}_1$  is a lattice vector and the brackets and overbar represent thermal and disorder averages respectively [7]. We have discussed the sharp increase in energy barriers (suggestive of an irreversibility line), and the onset of instabilities in the ordered phase according to a Lindemann criterion. One shortcoming of this model is its inability to verify the stability of the ordered phase with respect to large-wavelength fluctuations caused by point disorder. However, the stability of the Bragg Glass phase with respect to such fluctuations has recently been demonstrated [9]. Thus, this model should predict approximately when a given sample falls out of equilibrium, and when dislocations proliferate, although more sophisticated models are necessary to determine whether the dislocation proliferation occurs through a phase transition or a crossover.

The low temperature entanglement field  $B_m(0)$  should not be confused with the so called “decoupling field”  $H_\times \approx \Phi_0/(d^2 \gamma^2)$  for highly anisotropic HTSCs, above which a discretized version of Eqs. (26) and (27) should be used [29]. Vortex line behavior roughly independently in each Cu-O layer. The ratio of these two fields is

$$\frac{B_m(0)}{H_\times} \approx \gamma^2 c_L^{16/3} \left( \frac{d}{\xi} \right)^2 \left( \frac{\epsilon_0 \xi}{\gamma T^*} \right)^{10/3}. \quad (29)$$

For materials such as YBCO or BSCCO, this ratio is typically less than 1. A more detailed account of layering effects and the dispersive nature of the line tension is beyond the scope of this work.

We are indebted to E. Zeldov for stimulating our interest in this problem. We also benefited from helpful conversations with D. Huse, P. Le Doussal, C. Lieber and V. Vinokur. This work was supported by the National Science Foundation, primarily by the MRSEC program through Grant DMR-9400396 and in part through Grant DMR-9417047.

- 
- [1] J. G. Bednorz and K. A. Müller, Z. Phys. **64**, 189 (1986).
  - [2] G. Blatter *et al.*, Rev. Mod. Phys. **66**, 1125 (1994).
  - [3] D. R. Nelson and V. M. Vinokur, Phys. Rev. **B48**, 13 060 (1993).
  - [4] L. Balents and M. Kardar, Europhys. Lett. **23**, 503 (1993).
  - [5] A. I. Larkin, Sov. Phys. JETP **31**, 784 (1970); A. I. Larkin and Yu. N. Ovchinnikov, J. Low Temp. Phys. **34**, 409 (1979).

- [6] M. Feigelman, V. B. Geshkenbein, A. I. Larkin and V. M. Vinokur, Phys. Rev. Lett. **63**, 2303 (1989).
- [7] D. S. Fisher, M. P. A. Fisher and D. A. Huse, Phys. Rev. **B43**, 130 (1990).
- [8] J. A. Fendrich *et al.*, Phys. Rev. Lett. **74**, 1210 (1995).
- [9] T. Giamarchi and P. Le Doussal, Phys. Rev. Lett. **72**, 1530 (1994); Phys. Rev. **B52**, 1242 (1995); see also T. Nattermann, Phys. Rev. Lett. **64**, 2454 (1990), and J. Kierfeld, T. Nattermann and T. Hwa, cond-mat 9512101.
- [10] By “low” magnetic fields, we mean fields  $B$  smaller than the “decoupling field”  $H_\times \approx \Phi_0/(d^2 \gamma^2)$ , where  $\gamma^2 = m_z/m_\perp \gg 1$  is the mass anisotropy,  $\Phi_0 = hc/2e$  is the flux quantum, and  $d$  is the spacing between copper oxide planes. The fields considered here are nevertheless assumed to be large enough so that  $a_0 \leq \lambda$ , where  $a_0 = \sqrt{\Phi_0/B}$  is a typical vortex spacing and  $\lambda$  is the London penetration depth.
- [11] E. Zeldov *et al.*, Nature **375**, 373 (1995); see also H. Pastoriza *et al.*, Phys. Rev. Lett. **72**, 2951 (1994).
- [12] D. Majer, E. Zeldov and M. Konczykowski, Phys. Rev. Lett. **75**, 1166 (1995).
- [13] B. Khaykovich *et al.*, Phys. Rev. Lett. **76**, 2555 (1996).
- [14] M. Gingras and D. Huse, Lucent Technologies preprint.
- [15] R. Cubbit *et al.*, Nature (London) **365**, 407 (1993).
- [16] R. Wördenweber and P. Kes, Phys. Rev. **B34**, 494 (1986).
- [17] E. H. Brandt, Phys. Rev. **B34**, 6514 (1986); Jap. J. Appl. Phys. **26**, 1515 (1987).
- [18] T. Hwa *et al.*, Phys. Rev. Lett. **71**, 3545 (1993). Mechanical entanglement (with low crossing angles so that cutting barriers are large) would allow a few firmly pinned vortices to hold the others in place, similar to pinning of dislocation tangles in a work hardened metal.
- [19] S. Ryu, A. Kapitulnik and S. Doniach, Ohio State University preprint.
- [20] Proliferation of dislocations alone, without dissociation of the lines of disclination pairs buried in their core, would of course preserve the topological order of a hexatic glass. A subsequent crossover or phase transition would be required to produce a completely disordered glass. See, e. g., M. C. Marchetti and D. R. Nelson, Phys. Rev. **B42**, 9938 (1990).
- [21] T. Halpin-Healy and Y.-C. Zhang, Phys. Rep. **254**, 215 (1995), and references inside.
- [22] L. V. Mikheev, B. Drossel and M. Kardar, Phys. Rev. Lett. **75**, 1170 (1995).
- [23] T. Nattermann and R. Lipowsky, Phys. Rev. Lett. **61**, 2508 (1988).
- [24] D. R. Nelson and P. Le Doussal, Phys. Rev. **B42**, 10 113 (1990).
- [25] M. Tinkham, *Introduction To Superconductivity*, p. 165 (Reprint Edition, Krieger Publishing, Malabar, FL, 1980).
- [26] It should be stressed that, although useful for locating important physical phenomena in the phase diagram, the Lindemann criterion by itself cannot predict whether a given transition is first order, second order, or simply a crossover.
- [27] Since the mechanisms that generate dislocations are dif-

- ferent, the Lindemann parameters may not be identical for the melting and entanglement lines.
- [28] See the appendices in D. R. Nelson, in *The Vortex State*, 41–61, N. Bontemps *et al.* (eds.), Kluwer Academic Publishers, the Netherlands (1994).
- [29] S. Ryu, A. Kapitulnik and S. Doniach, Phys. Rev. Lett. **71**, 4245 (1993); A. E. Koshelev, P. Le Doussal and V. Vinokur, Phys. Rev. **B53**, R8855 (1996).